

# Raman spectra in iron-based quaternary $\text{CeO}_{1-x}\text{F}_x\text{FeAs}$ and $\text{LaO}_{1-x}\text{F}_x\text{FeAs}$

S. C. Zhao,<sup>1</sup> D. Hou,<sup>2,1</sup> Y. Wu,<sup>3</sup> T. L. Xia,<sup>1</sup> A. M. Zhang,<sup>1</sup> G. F. Chen,<sup>4</sup>  
J. L. Luo,<sup>4</sup> N. L. Wang,<sup>4</sup> J. H. Wei,<sup>1</sup> Z. Y. Lu,<sup>1</sup> and Q. M. Zhang<sup>1,3,\*</sup>

<sup>1</sup>*Department of Physics, Renmin University of China, Beijing 100872, P. R. China*

<sup>2</sup>*Department of Physics, Shandong University, Jinan 250100, P. R. China*

<sup>3</sup>*National Laboratory of Solid State Microstructures,*

*Department of Physics, Nanjing University, Nanjing 210093, P. R. China*

<sup>4</sup>*Beijing National Laboratory for Condensed Matter Physics, Institute of Physics,  
Chinese Academy of Sciences, Beijing 100080, P. R. China*

(Dated: November 12, 2018)

## Abstract

Raman spectra have been measured on iron-based quaternary  $\text{CeO}_{1-x}\text{F}_x\text{FeAs}$  and  $\text{LaO}_{1-x}\text{F}_x\text{FeAs}$  with varying fluorine doping at room temperatures. A group analysis has been made to clarify the optical modes. Based on the first principle calculations, the observed phonon modes can be assigned accordingly. In  $\text{LaO}_{1-x}\text{F}_x\text{FeAs}$ , the  $E_g$  and  $A_{1g}$  modes related to the vibrations of La, are suppressed with increasing F doping. However F doping only has a small effect on the  $E_g$  and  $A_{1g}$  modes of Fe and As. The Raman modes of La and As are absent in rare-earth substituted  $\text{CeO}_{1-x}\text{F}_x\text{FeAs}$ , and the  $E_g$  mode of oxygen, corresponding to the in-plane vibration of oxygen, moves to around  $450\text{ cm}^{-1}$  and shows a very sharp peak. Electronic scattering background is low and electron-phonon coupling is not evident for the observed phonon modes. Three features are found above  $500\text{ cm}^{-1}$ , which may be associated with multi-phonon process. Nevertheless it is also possible that they are related to magnetic fluctuations or interband transitions of d orbitals considering their energies.

PACS numbers: 78.30.-j, 63.20.D-, 74.25.Kc

## I. INTRODUCTION

The discovery of iron-based superconductors has stimulated many interests in searching higher- $T_c$  superconductors without copper-oxide planes. Soon after the first  $\text{LaO}_{1-x}\text{F}_x\text{FeAs}$  was reported with  $T_c=26$  K<sup>1</sup>, rare-earth substitution compounds  $\text{SmO}_{1-x}\text{F}_x\text{FeAs}$  and  $\text{CeO}_{1-x}\text{F}_x\text{FeAs}$  were synthesized and their  $T_c$ 's can go up to above 40 K<sup>2,3</sup>. For  $\text{LaO}_{1-x}\text{F}_x\text{FeAs}$ ,  $T_c$  can be raised to above 40 K under high pressure<sup>23</sup>. A higher  $T_c$  of 52 K in Fe-based series superconductors was reported in  $\text{PrO}_{1-x}\text{F}_x\text{FeAs}$  which was synthesized under high pressure<sup>4</sup>. The measurements of Hall coefficients indicates that the carriers in the superconductors are electron-like. On the other hand, hole-doped  $(\text{La, Sr})\text{O}_{1-x}\text{F}_x\text{FeAs}$  was synthesized successfully with  $T_c=26$  K<sup>6</sup>. Transition-metal substituted  $\text{LaO}_{1-x}\text{F}_x\text{NiAs}$  was also reported with  $T_c=4$  K and an extremely sharp superconducting transition<sup>7</sup>. Most recently, a very exciting result shows that a maximum  $T_c$  of 55K can be obtained even without F doping in the Fe-based superconductors<sup>8</sup>. Up to now the record of the highest  $T_c$  56.5 K in iron-based superconductors was archived in  $\text{Gd}_{1-x}\text{Th}_x\text{OFeAs}$  without F doping<sup>9</sup>. It is believed that electrons are transferred into FeAs conducting layers effectively by  $\text{Th}^{4+}$  substitution of  $\text{Gd}^{3+}$ , just like F doping. This means that carrier concentration and superconducting transition temperature can be controlled and tuned by oxygen content and rare-earth substitution, which is much similar to the case of cuprate superconductors. A very high upper critical field over 100T was estimated by resistance measurements under high magnetic field, even exceeding that of cuprate superconductors<sup>22</sup>.

The early band structure calculations suggested that the pure  $\text{LaOFeAs}$  compound is a nonmagnetic metal but with strong ferromagnetic or antiferromagnetic (AFM) instability<sup>18</sup>. Later, it was found that the antiferromagnetically ordered state<sup>10,11</sup> has a lower energy than the nonmagnetic one, due to the Fermi surface nesting<sup>11</sup>. It was then<sup>14</sup> predicted that the AFM state should form a striped structure by breaking the rotational symmetry, which was indeed observed by the neutron scattering experiment<sup>12,13</sup>. The further theoretical studies show that the superexchange antiferromagnetic interaction between the next nearest neighbor Fe-Fe bridged by As is responsible for the stripe-ordered Fe moments<sup>19,20</sup>. Some microscopic models have been constructed to understand the superconductivity in the compounds with iron-arsenite plane instead of copper-oxygen plane. There is no consensus on some important issues such as pairing mechanism and symmetry yet. More experimental

efforts and further theoretical considerations are needed to reveal the properties of ground state and magnetic excitations.

For the parent compounds without F doping, a subtle structural change and a successive magnetic transition were revealed by means of transport measurements, specific heat and neutron scattering etc. It is still a key issue to understand the connection between the structural change and magnetic transition. Furthermore, exploring the driving force for pairing requires a basic knowledge on some important interactions such as electron-phonon coupling. So it is important and necessary to learn more detailed information on lattice vibrations in the compounds. Raman scattering is known as a unique technique in studying optical phonon modes. Besides, if allowed by selection rules, it is possible to obtain additional information about magnetic, electronic and other collective excitations. In fact, a nice Raman scattering study on iron-based materials has been done on ab plane of single crystal grain by microscopic Raman method<sup>15</sup>. However the spectra only covered 100 to 400  $\text{cm}^{-1}$  and in-plane vibrations were not resolved due to the limit of ab plane.

In this paper, Raman scattering measurements at room temperature from 30 to 2000  $\text{cm}^{-1}$ , have been performed on two kinds of iron-based materials  $\text{CeO}_{1-x}\text{F}_x\text{FeAs}$  with  $x=0$  ( $T_c=0$  K) and 0.16( $T_c=41$  K), and  $\text{LaO}_{1-x}\text{F}_x\text{FeAs}$  with  $x=0$  ( $T_c=0$  K), 0.04( $T_c=17$  K) and  $x=0.08$  ( $T_c=26$  K), respectively. Six Raman phonon modes were observed below 500  $\text{cm}^{-1}$ . Based on the structural data obtained by neutron scattering and X-ray diffraction, a group analysis was made to classify the optical modes. Then first-principle calculations were carried out to calculate the optical modes at  $\Gamma$  point. By comparison with the calculations and group analysis, the observed phonon modes were assigned accordingly. The changes of some modes with F doping and rare-earth substitution were discussed. And electron-phonon coupling was found to be small. Three weak features were observed above 500  $\text{cm}^{-1}$ , which may be associated with multi-phonon process, magnetic fluctuations or interband transitions.

## II. EXPERIMENTAL DETAILS

Polycrystal samples of  $\text{CeO}_{1-x}\text{F}_x\text{FeAs}$  and  $\text{LaO}_{1-x}\text{F}_x\text{FeAs}$  were synthesized by solid state reaction method. As precursor materials, CeAs or LaAs were presynthesized by reacting Ce or La chips and As pieces in an evacuated quartz tube. Then FeAs was obtained with a similar process. Using CeAs/LaAs, Fe,  $\text{CeO}_2/\text{La}_2\text{O}_3$ ,  $\text{CeF}_3/\text{LaF}_3$  and FeAs as starting ma-

terials, the raw materials with stoichiometric ratio were mixed thoroughly and pressed into pellets. The pellets were warped with Ta foil and sealed in an evacuated quartz tube. Almost pure phase polycrystal samples were obtained after annealing. The detailed procedure for preparing the samples can be found elsewhere<sup>3</sup>. The temperature dependence of susceptibility and resistivity of the polycrystal samples used in the present Raman study is shown in Fig. 1. The transition temperature width shows the high quality of the samples. For  $\text{CeO}_{1-x}\text{F}_x\text{FeAs}$ , many shining single crystal grains can be seen even without a microscope. After polishing, a flat alloy-like surface can be obtained. Unfortunately Raman signal is too weak to be detected because most intensities of excitation light were reflected back by the alloy-like surface. In order to increase the intensities of incident light effectively and to resolve more phonon modes beyond ab plane, the present Raman measurements were done with ground fine powder.

The Raman measurements were performed with a triple-grating monochromator (Jobin Yvon T64000), which works with a microscopic Raman configuration. A  $50\times$  objective microscopic lens with a working distance of 10.6 mm, is used to focus the incident light on sample and collect the scattered light from sample. The detector is a back-illuminated CCD cooled by liquid nitrogen. An solid-state laser (Laser Quantum Torus 532) with high-stability and very narrow width of laser line, is used with an excitation wavelength of 532 nm. The laser beam of 3 mW was focused into a spot of less than 10 microns in diameter on sample surface.

### III. ASSIGNMENT OF RAMAN PHONONS

The refined structure parameters of  $\text{LaOFeAs}$  have been obtained by neutron scattering and X-ray diffraction. It has a tetragonal  $\text{ZrCuSiAs}$ -type structure with space group  $P4/nmm$  (No. 129, origin choice 2) and point group  $D_{4h}$ . Atoms La, O/F, Fe and As occupy

Table I: Classifications of optical modes of  $\text{LaOFeAs}$

Atom	Wyckoff position	Raman modes	IR modes
La	2c	$A_{1g}+E_g$	$A_{2u}+E_u$
O/F	2a	$B_{1g}+E_g$	$A_{2u}+E_u$
Fe	2b	$B_{1g}+E_g$	$A_{2u}+E_u$
As	2c	$A_{1g}+E_g$	$A_{2u}+E_u$

Wyckoff positions 2c, 2a, 2b and 2c, respectively. Symmetry analysis shows that there are eight Raman-active modes and six infrared(IR)-active modes, as classified in Table I.

Table II: Assignment of optical phonons in comparison with the first-principle calculations. The cited data of IR phonons comes from ref. 14. Just the dominant atoms involved in a specific mode are listed here. The last column describes the approximate direction and phase of vibration, where [100], [010], [001] are parallel to the a, b, c crystal axis, respectively. See FIG. 3 for the crystal coordinate system.

Experimental ( $\text{cm}^{-1}$ )	Calculated ( $\text{cm}^{-1}$ )	Symmetry	Active	Atom	Vibration
	60.95657	$E_u$	IR	La, As, Fe	[100] or [010]
97	80.73106	$A_{2u}$	IR	La, As, Fe	[001]
96	111.02250	$E_g$	Raman	La	[100] or [010], out-of-phase
137	138.06264	$E_g$	Raman	As, Fe	[110] or [1-10], out-of-phase
161	180.56708	$A_{1g}$	Raman	La	[001], out-of-phase
	203.74154	$A_{1g}$	Raman	As	[001], out-of-phase
214	218.21930	$B_{1g}$	Raman	Fe	[001], out-of-phase
248	254.15852	$A_{2u}$	IR	Fe, As	[001]
266	268.08770	$E_u$	IR	Fe, As	[100] or [010]
278	279.24677	$E_g$	Raman	Fe	[110] or [1-10], out-of-phase
	280.21650	$E_u$	IR	O	[100] or [010], in-phase
	282.44946	$B_{1g}$	Raman	O	[001], out-of-phase
338	388.45420	$A_{2u}$	IR	O	[001], in-phase
423	420.80567	$E_g$	Raman	O	[100] or [010], out-of-phase

To assign the phonon modes at  $\Gamma$ -point, the phonon frequencies of non-magnetic LaOFeAs crystal have been calculated in the framework of the density perturbation functional theory (DFPT) using plane-wave pseudopotentials<sup>16</sup> with the generalized gradient approximation (GGA) of Perdew-Burke-Ernzerh (PBE)<sup>17</sup> for the exchange-correlation potentials. Firstly, a self-consistent calculation was accomplished using the experimental lattice parameters and the energy minimized internal atomic positions<sup>11</sup>, during which the following parameters were adopted: the 45 and 360 Ryd cutoffs of kinetic energy for wave-function and charge-

density, respectively; the  $24 \times 24 \times 12$  uniform k-space for the k-points integration; and the gaussian smearing parameter of 0.002 Ryd. Then, by diagonalizing the dynamical matrix generated from converged potentials, we obtained the eigenvalues, namely the squared phonon frequencies, and the eigenvectors to derive the displacements of each atom in a specific vibration mode.

Eight frequency-distinguishable Raman-active phonon modes were deduced at  $\Gamma$ -point, consisting of four two-fold degenerated  $E_g$ , two non-degenerated  $A_{1g}$  and two non-degenerated  $B_{1g}$  modes, which consists with the group symmetry analysis. Comparing them to above Raman spectra showed a fairly good agreement, see Fig. 2 and Tab. II. All the Raman active vibration modes are characterized in Fig. 3, where the arrows indicate the vibration directions of the corresponding atoms, with their lengths representing the relative vibration amplitude compared with those of other atoms in the same mode.

#### IV. DISCUSSIONS

In Fig. 2, at first glance LaOFeAs system has a similar phonon spectrum for different F doping. There is no obvious frequency shift or change of peak shape for the three samples. However there still exist some small changes with varying F doping. Both  $E_g$  mode at  $96 \text{ cm}^{-1}$  and  $A_{1g}$  mode at  $161 \text{ cm}^{-1}$  of La are suppressed gradually with increasing F doping. It can be naturally understood as the effect of F dopants entering LaO layer. The sensitivity of La phonon modes to F doping, may be considered as an alternative way to characterize the concentration of F doping.

F doping has little effect on the Fe and As-dominated phonon modes, such as  $B_{1g}$  mode at  $214 \text{ cm}^{-1}$  and  $E_g$  mode at  $278 \text{ cm}^{-1}$  of Fe, and  $E_g$  mode at  $137 \text{ cm}^{-1}$  of As. The fact can be easily explained because F dopants are far away from FeAs layer and thus has little effect on Fe and As-related vibrations. These three modes have a special significance in exploring the mechanism of magnetic phase transition near 140 K revealed by some experiments. As suggested by neutron scattering and other measurements, there also exists a structural changes just above the temperatures of magnetic phase transition. For iron-based superconductors, it is still a key issue to make clear whether there is a connection between the magnetic transition and structural change or not. The modes related to Fe and As would play an important role in answering the above question in further Raman

scattering measurements at various temperatures and with applied magnetic field.

A relatively broad  $E_g$  mode of oxygen was observed near  $423\text{ cm}^{-1}$  for LaOFeAs. We will come back to this point in combination with the results of CeOFeAs in the following.

A striking change in the Raman spectra of CeOFeAs is that the  $E_g$  phonon of oxygen becomes very strong and moves to  $450\text{ cm}^{-1}$ . The reason for the sharper oxygen  $E_g$  mode can be originated from a better sample quality of CeOFeAs as described above. Interestingly, Infrared measurements also observed a mode with quite high intensities near  $430\text{ cm}^{-1}$  in both LaOFeAs and CeOFeAs, which moves to higher frequencies with decreasing temperatures, showing a typical phonon behavior<sup>3,14</sup>. However, the first principle calculations show that there should be no IR-active mode above  $400\text{ cm}^{-1}$ . It is speculated that an inversion symmetry breaking can cause an intensity leakage of oxygen  $E_g$  mode into IR channel. If it is true, that means that a subtle structural distortion could occur even at room temperatures.

The other change is that the modes below  $200\text{ cm}^{-1}$  contributed by La and As, can not be observed. This may be caused by the distortion of LaO layer due to the substitution of La by smaller Ce ions. The Raman results based on single crystal are needed to confirm this point.

Besides the above first-order Raman phonons, there exist some common features above  $500\text{ cm}^{-1}$  in both LaOFeAs and CeOFeAs, which are located at  $590\text{ cm}^{-1}$ ,  $846\text{ cm}^{-1}$  and  $1300\text{ cm}^{-1}$ . Generally, these features originate from multi-phonon processes. For instance, the feature at  $846\text{ cm}^{-1}$  can be contributed by two  $E_g$  phonons of oxygen simply considering its frequency. On the other hand, the energies of features correspond to 73, 105 and 161 meV, respectively. They are close to the interband differences of d orbitals<sup>21</sup>, and also the ferromagnetic/antiferromagnetic exchange energies according to electronic structure calculations<sup>11,20</sup>. At present it can not be ruled out that some of the features are associated with the interband transitions or magnetic fluctuations. Further Raman experiments under applied magnetic field could be helpful to answer this question.

Although polycrystal samples were used in the present measurements, it can be seen that electronic scattering background is low. And for the observed modes, especially those of Fe and As, it is not easy to distinguish evident features of electron-phonon coupling. The measurements on single crystal are necessary in the further study on electronic Raman scattering.

## V. CONCLUSIONS

In summary, Raman measurements of newly discovered iron-based superconductors have been performed at room temperatures. The observed phonon modes are assigned in combination with symmetry analysis and first-principle calculations. The phonon modes are discussed in detail. The assignment will provide a basis for further study on structural and electronic properties and exploring the superconductivity in the high- $T_c$  materials. Besides the first-order Raman phonons, more features found at higher frequencies may be related to magnetic excitations or interband transitions.

## VI. ACKNOWLEDGMENTS

The work was supported by the MOST of China (973 project No.:2006CB601002d & 2006CB9213001) and NSFC Grant No. 10574064 & 20673133.

---

\* Electronic address: qmzhang@ruc.edu.cn

- <sup>1</sup> Y. Kamihara, T. Watanabe, M. Hirano, and H. Hosono, *J. Am. Chem. Soc.* **130**, 3296 (2008).
- <sup>2</sup> X. H. Chen, T. Wu, G. Wu, R. H. Liu, H. Chen and D. F. Fang, arXiv: 0803.3603v1; *Nature advance online publication*, doi:10.1038/nature07045 (25 May 2008).
- <sup>3</sup> G. F. Chen, Z. Li, D. Wu, G. Li, W. Z. Hu, J. Dong, P. Zheng, J. L. Luo, and N. L. Wang, arXiv: 0803.3790v2.
- <sup>4</sup> Zhi-An Ren, Jie Yang, Wei Lu, Wei Yi, Guang-Can Che, Xiao-Li Dong, Li-Ling Sun, Zhong-Xian Zhao, arXiv:0803.4283.
- <sup>5</sup> Xiyu Zhu, Huan Yang, Lei Fang, Gang Mu, Hai-Hu Wen, arXiv:0803.1288v1.
- <sup>6</sup> H. H. Wen, G. Mu, L. Fang, H. Yang, and X. Y. Zhu, *EuroPhys. Lett.* **82**, 17009 (2008).
- <sup>7</sup> Z. Li, G. F. Chen, J. Dong, G. Li, W. Z. Hu, J. Zhou, D. Wu, S. K. Su, P. Zheng, N. L. Wang and J. L. Luo, arXiv: 0803.2572v1.
- <sup>8</sup> Zhi-An Ren, Guang-Can Che, Xiao-Li Dong, Jie Yang, Wei Lu, Wei Yi, Xiao-Li Shen, Zheng-Cai Li, Li-Ling Sun, Fang Zhou, Zhong-Xian Zhao, arXiv:0804.2582.
- <sup>9</sup> Cao Wang, Linjun Li, Shun Chi, Zengwei Zhu, Zhi Ren, Yuetao Wang, Xiao Lin, Yongkang luo, Xiangfan Xu, Guanghan Cao, and Zhu'an Xu, arXiv:0804.4290v1.



- <sup>10</sup> Chao Cao, P. J. Hirschfeld, and Hai-Ping Cheng, arXiv:0803.3236v1.
- <sup>11</sup> Fengjie Ma, Zhong-Yi Lu, arXiv:0803.3286v1.
- <sup>12</sup> Clarina de la Cruz, Q. Huang, J. W. Lynn, Jiying Li, W. Ratcliff II, J. L. Zarestky, H. A. Mook, G. F. Chen, J. L. Luo, N. L. Wang, Pengcheng Dai, arXiv: 0804.0795; *Nature advance online publication*, doi:10.1038/nature07057 (25 May 2008).
- <sup>13</sup> M. A. McGuire, A. D. Christianson, A. S. Sefat, R. Jin, E. A. Payzant, B. C. Sales, M. D. Lumsden, D. Mandrus, arXiv: 0804.0796v1.
- <sup>14</sup> J. Dong, H. J. Zhang, G. Xu, Z. Li, G. Li, W. Z. Hu, D. Wu, G. F. Chen, X. Dai, J. L. Luo, Z. Fang, and N. L. Wang, arXiv: 0803.3426v1.
- <sup>15</sup> V. G. Hadjiev, M. N. Iliev, K. Sasmal, Y. -Y. Sun, and C. W. Chu, arXiv: 0804.2285v1.
- <sup>16</sup> P. Giannozzi et al., <http://www.quantum-espresso.org> .
- <sup>17</sup> J. P. Perdew, K. Burke, and M. Ernzerhof, Phys. Rev. Lett. 77, 3865,(1996).
- <sup>18</sup> D.J. Singh and M.H. Du, cond-mat/0803.0429; G. Xu, W. Ming, Y. Yao, X. Dai, and Z. Fang, cond-mat/0803.1282; K. Haule, J.H. Shim, and G. Kotliar, cond-mat/0803.1279.
- <sup>19</sup> T. Yildirimar, cond-mat/0804.2252.
- <sup>20</sup> F.J. Ma, Z.Y. Lu, and T. Xiang, cond-mat/0804.3370.
- <sup>21</sup> K. Haule and G. Kotliar, cond-mat/0805.0722v1.
- <sup>22</sup> F. Hunte, J. Jaroszynski, A. Gurevich, D. C. Larbalestier, R. Jin, A. S. Sefat, M. A. McGuire, B. C. Sales, D. K. Christen AND D. Mandrus, *Nature advance online publication*, doi:10.1038/nature07058 (25 May 2008).
- <sup>23</sup> H. Takahashi, K. Igawa, K. Arii, Y. Kamihara, M. Hirano, and H. Hosono, Nature **453**, 376 (2008).

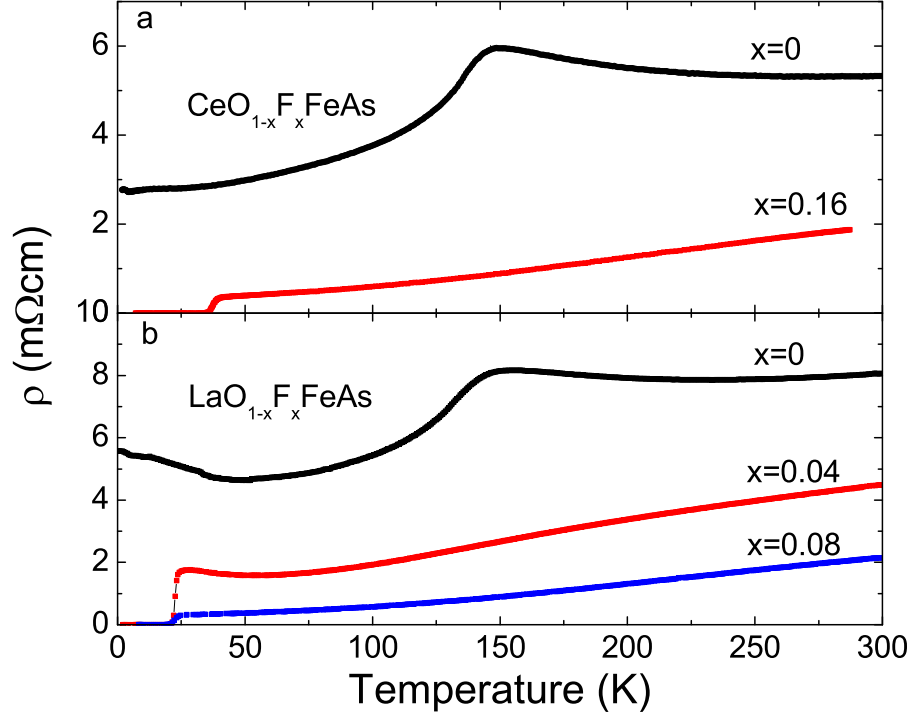


FIG. 1: (color online) Temperature dependence of resistivity for (a)  $\text{CeO}_{1-x}\text{F}_x\text{FeAs}$  and (b)  $\text{LaO}_{1-x}\text{F}_x\text{FeAs}$  used in the present Raman measurements. The sharp superconducting transitions indicate the high-quality of samples. Especially for the superconducting  $\text{CeO}_{1-x}\text{F}_x\text{FeAs}$ , it shows a quite small residual resistivity by extrapolation.

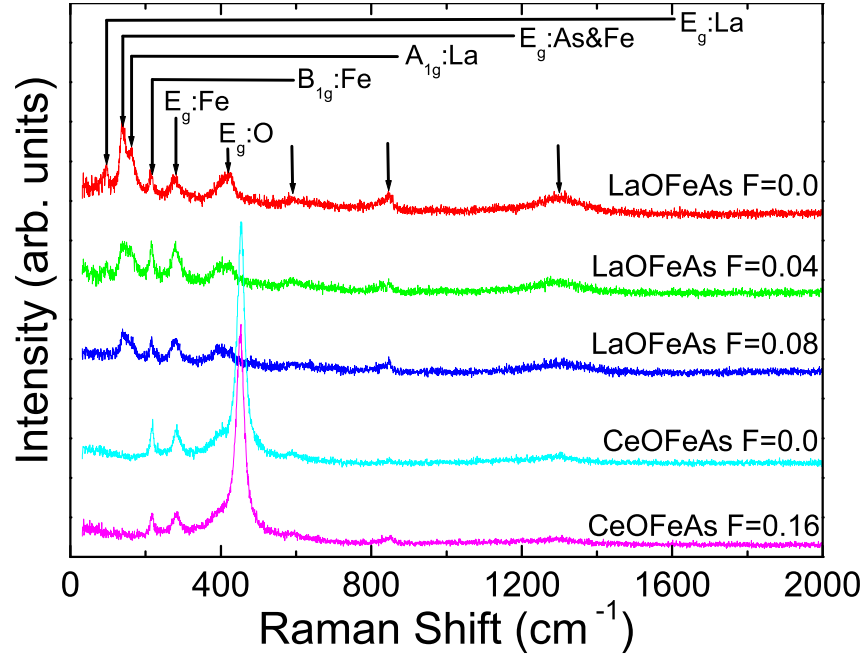


FIG. 2: (color online) Raman spectra of  $\text{CeO}_{1-x}\text{F}_x\text{FeAs}$  and  $\text{LaO}_{1-x}\text{F}_x\text{FeAs}$  at room temperatures.

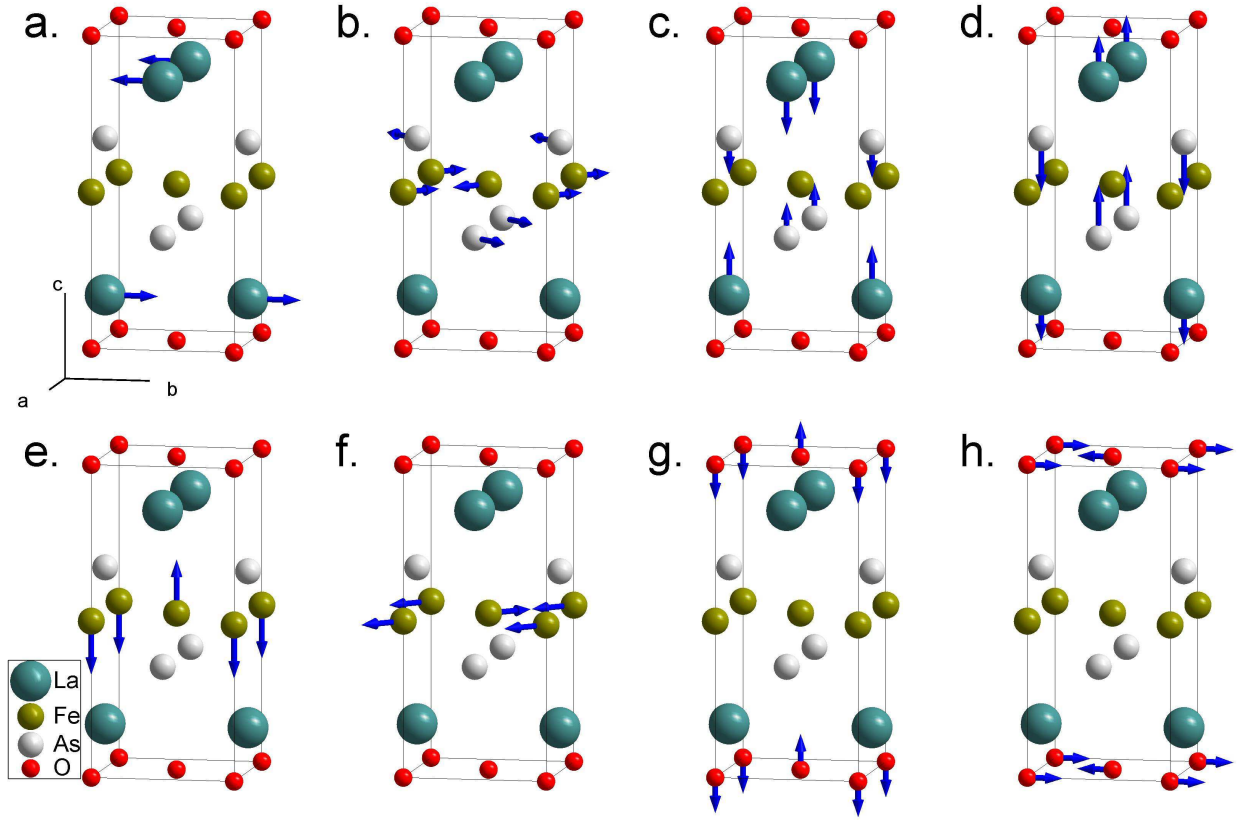


FIG. 3: (color online) Eight Raman-active modes of LaOFeAs: (a) $E_g$  of La ( $96 \text{ cm}^{-1}$ ); (b) $E_g$  of As & Fe ( $137 \text{ cm}^{-1}$ ); (c) $A_{1g}$  of La ( $161 \text{ cm}^{-1}$ ); (d) $A_{1g}$  of As (not observed); (e) $B_{1g}$  of Fe ( $214 \text{ cm}^{-1}$ ); (f) $E_g$  of Fe ( $278 \text{ cm}^{-1}$ ); (g) $B_{1g}$  of O (not observed); (h) $E_g$  of O ( $423 \text{ cm}^{-1}$ ).